Mucoadhesion of Latexes. I. Analytical Methods and Kinetic Studies

Carlo Durrer,[1] Juan Manuel Irache,[1] Francis Puisieux,[1] Dominique Duchêne,[1] and Gilles Ponchel[1,2]

Received August 19, 1993; accepted November 30, 1993

A Fourier transform infrared spectroscopy/attenuated total reflection technique for direct quantification of adsorbed poly(styrene) latexes on rat intestinal mucosa was developed for deposited latex amounts up to 1.5 g/m^2. The method agreed well with another dosage assay of adsorbed particles by turbidimetry after denaturation of the mucus. Adsorption kinetics were made under static conditions at latex concentrations of 4 g/L in physiological saline. Ninety percent of equilibrium was reached after 10 min for a particle size of 230 nm, 20 min for a size of 320 nm, and 30 min for a size of 670 nm. The plateaus were between 0.6 and 0.9 g/m^2 (adsorbed mass per apparent surface of mucosa). The first phase of the kinetics was theoretically approached by a diffusion model in the suspension medium. Mucosa from rat jejunum and ileum could be considered as a homogeneous biological model for latex adsorption.

KEY WORDS: mucoadhesion; bioadhesion; latex; infrared spectroscopy; adsorption; nanoparticle.

INTRODUCTION

Mucoadhesion is the attachment of synthetic or natural polymers to a mucous membrane (1), and it is defined in terms of the energy involved in the formation of the adhesive junction. The surfaces are considered to be adhered when work is required to separate them to their original state (2).

On the one hand, bioadhesion of tablets was evaluated in tensile experiments measuring the maximal detachment force and the apparent adhesion work required to separate these forms from a mucous membrane (3,4). On the other, experiments using desorption by a flowing liquid film to test mucoadhesion of microparticles (5) or nanoparticles (6) gave good comparative results but little information about the interfacial forces involved. In another paper (7), the adsorption of particles from the flowing film of a dilute latex suspension on to the mucous surface of an intestinal strip was studied. The steady-state fraction of adsorbed particles was related to the length of the intestinal strip, the flow rate, and a mass transfer coefficient depending theoretically on the diffusion of the latex particles in the liquid film and a collision barrier factor. However, in an open biological system, although steady-state condition may be encountered, the quantitative evaluation will always be very complex.

Therefore, we decided to develop a new model to evaluate mucoadhesion by considering physicochemical interactions between latexes and mucosa under equilibrium conditions. The aim of the present work was to elaborate analytical methods for the adsorption of nonlabeled model particles and to determine by kinetic studies the time necessary to reach equilibrium of adsorption, which is the first essential element for the subsequent investigation of adsorption isotherms. Finally, the biological model was validated.

MATERIALS AND METHODS

Poly(styrene) Latexes

Poly(styrene) latexes were chosen as a model colloidal system. A plain nonmodified (PSL-650*) and a carboxylate (CML-350*) poly(styrene) latex were provided by Polymer Laboratories, Church Stretton, Shropshire, UK. Both latexes contained a surfactant (indicated by a superscript asterisk). From manufacturing process, a fatty acid-type surfactant was adsorbed on PSL-650* and sodium dodecyl sulfate (SDS) on CML-350*. Surfactant-free latexes were supplied as Polybead Carboxylate Microspheres (PCM-200, PCM-750, PCM-1000) by Polysciences, Eppelheim, Germany. The number in the latex designation indicates the nominal particle size (nm). The sizes were verified by a Coulter submicron particle analyzer N4MD (Coultronics, Margency, France). The weight diameters are listed in Table I. The latex concentrations were determined by turbidimetry (8).

Mucosa Samples

As a model mucosa, the fresh small intestine of sacrificed male Wistar rats (IFFA CREDO, L'Arbresle, France) was excised, rinsed with physiological saline (NaCl 0.9%), and cut into segments of 5-cm length. Each segment was then opened lengthwise along the mesentery with scissors and spread on a glass slide that was previously covered with an aluminium film. A plate of aluminium with a slit in the center was then fixed on the so-prepared mucosa samples (Fig. 1). For the present study, the slit was placed between Peyer's patches to avoid segmental differences, since Peyer's patches were reported to internalize particulate matter (9).

Latex Deposition on Mucosa

For infrared standard curves, the mucosa in the slit of the aluminium device was covered with 50 μL of latex dilutions. The water was evaporated at room temperature, and the samples were dried at 50°C. The deposited latex amount was expressed as a mass of polymer per apparent surface of mucosa (g/m^2). For the comparison of IR and turbidimetric analysis, 1 mL of physiological saline with certain latex concentrations was put into the slit during 30 min. Finally, for the kinetic studies and the validation of the mucosa as biological model, the latex bulk concentration was fixed at 4 g/L. All experiments were conducted at room temperature. After the contact time, the latexes were sucked off and the samples were rinsed with 5 mL of NaCl 0.9% to eliminate nonattached particles. The adsorbed amount was measured

[1] Centre d'Etudes Pharmaceutique, URA CNRS 1218, Université Paris-Sud, 92296 Châtenay-Malabry, France.

[2] To whom correspondence should be addressed at Laboratoire de Pharmacie Galénique et de Biopharmacie, Université Paris-Sud, 5 rue Jean-Baptiste Clément, F-92296 Châtenay-Malabry, France.

0724-8741/94/0500-0674$07.00/0

Table I. Analytical Characteristics of Latexes

Latex	$D_w \pm$ SD (nm)[a]	Ratio (T/IR)[b]
PCM-200	230 ± 13	1.185
CML-350*	320 ± 26	1.019
PSL-650*	670 ± 80	0.865
PCM-750	711 ± 24	1.189
PCM-1000	875 ± 40	1.022

[a] D_w, weight diameter by photon correlation spectroscopy.
[b] Ratio of turbidimetric data to infrared data.

either by Fourier transform infrared spectroscopy, combined with the attenuated total reflection technique (FTIR-ATR), or by turbidimetry.

Turbidimetric Analysis

For turbidimetric measurements, the mucous layer including the adsorbed particles was scraped off the membrane with a microspatula and dispersed in 10 mL of a solution with 1% sodium hydroxyde (NaOH) and 2% SDS. The samples were treated for 2 hr in a Branson 5200 ultrasonication bath (Bioblock Scientific, Illkirch, France) and left overnight at room temperature until the mucus was completely dissolved, and the turbidity of the latex was measured.

FTIR-ATR Analysis

For IR measurements, the dried mucosa samples including the backing film of aluminium were separated from the glass slides and spread, without any further sample preparation, onto the zinc selenide (ZnSe) crystal of the flat sampling plate of the ATR accessory (Specac Limited, Orpington, Kent, UK). As shown previously (10), the good contact between the sample and the crystal required for this technique was obtained using a special adjustable pressure device of the ATR accessory. The samples were run on a Mattson 5000 FT-IR spectrometer (Unicam, Cambridge, UK) equipped with a MCT detector. The measurements were made under ambient laboratory conditions. The sampling conditions were set for 75 scans at 2-cm^{-1} resolution, so that rapid data acquisition, within 1 min, and a good signal/noise ratio were obtained. For quantitative analysis, the peak of poly(styrene) at 1493 cm^{-1} and the amide II peak (Fig. 2) were integrated to their base (peak surface), and the surface-to-surface ratio (latex/mucus) of these peaks was used to express the latex amount deposited on the mucosa surface

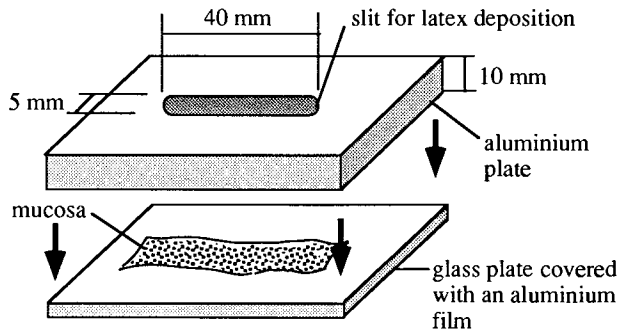

Fig. 1. Device for the deposition of latexes onto the mucosa.

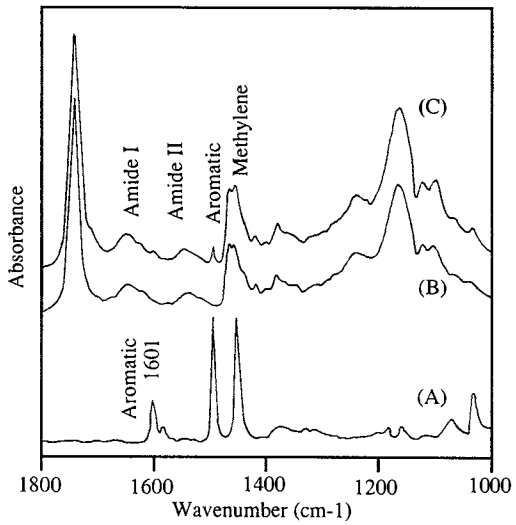

Fig. 2. FTIR-ATR spectra of poly(styrene) latex (A) and mucosa samples with (C) and without (B) deposited latex (PSL-650*), respectively. Deposited amount, 5 g/m^2.

(10). The ratios were then plotted as a function of the deposited latex amounts, and linear regression between 0 and 1.5 g/m^2 led to a standard curve for each latex. The samples from adsorption studies were then quantified by means of these standard curves.

RESULTS

IR Spectra

Figure 2 shows IR spectra of nonmodified poly(styrene) latex and mucosa sample with and without latex. The very strong carbonyl peak of absorbance at 1746 cm^{-1} in the mucosa spectrum (Fig. 2B) originated mainly from the C=O stretching vibration of the carbohydrates of the glycoprotein in the mucous layer, since the dry mucus of the rat small intestine consists of 72% carbohydrates, 12% proteins, and less than 0.1% lipids (11). When the pressure on the sample was increased by the pressure device of the ATR accessory, this peak increased strongly (10). The CH_2- and CH_3-deformation vibrations at 1467 cm^{-1} showed the same dependence on the sampling pressure. Contrary to these bands of absorbance, the peaks in the amide I band around 1646 cm^{-1} (carbonyl stretching vibration) and in the amide II band around 1542 cm^{-1} (N-H deformation vibration) displayed less dependence on sampling pressure. The spectrum of poly(styrene) latex (Fig. 2A) showed very typical peaks of aromatic vibration at 1601 and at 1493 cm^{-1}. The latex particles also absorbed in the methylene band, as did the mucosa, but with a maximum at 1453 cm^{-1}. The spectra of mucosa and latex were then compared with the spectra of samples in which latex particles were deposited on the mucosa surface (Fig. 2C). In fact, the peaks in the aromatic bands (1601 and 1493 cm^{-1}) and in the methylene band at 1453 cm^{-1} allowed the detection of the presence of the latexes at the surface of mucosa. The poly(styrene) peak at 1601 cm^{-1} was quite strongly superposed by the amide I absorbance of the mucus, and the methylene peak of the latex at 1453 cm^{-1} displayed a more intensive shoulder of

the mucus peak at 1467 cm^{-1}, whereas the aromatic peak at 1493 cm^{-1} was situated at a frequency without any specific mucus absorbance. Comparing the spectra of the same sample at different sampling pressures, it was seen that the amide II band and the poly(styrene) peak (1493 cm^{-1}) next to it depended just slightly and in the same manner on the sampling pressure (10). The IR absorbance of the amide II and the latex peaks was always far from saturation (absorbance $\approx$ 0.05).

Comparison of IR and Turbidimetric Results

Samples from adsorption experiments performed under the same conditions were quantified by FTIR-ATR or turbidimetry. The results are compared in Fig. 3. Theoretically, the same results would have been found by both techniques, and therefore, the ratios (adsorption by turbidimetry/adsorption by IR) would have been equal to 1 and situated on the bisection line. The experimental ratios are represented in Table I.

Adsorption Kinetics

The studies of latex adsorption versus time are represented in Fig. 4. The adsorption was very rapid for all three latexes during the initial time period (0 to 1 min) and was then followed by a period of decreasing rate of adsorption. Ninety percent of the plateau level was reached after 10 min for PCM-200, 20 min for CML-350*, and 30 min for PSL-650*. The estimated final adsorption values were taken from the mean values in the plateaus of the near-equilibrium adsorption isotherms (12), as proposed by Vincent *et al.* (13).

For high-affinity adsorption, implying irreversibility, where desorption may be neglected, a mathematical model based on Langmuir analysis for molecular adsorption was proposed (13,14). For the present kinetic study, it was considered that the particles which resisted the washout were adsorbed irreversibly (12). Thus, the concentration C (g/L) of unadsorbed particles was written as a function of time t (min):

$$dC(t)/dt = -KC(t)\,[1-q(t)] \qquad (1)$$

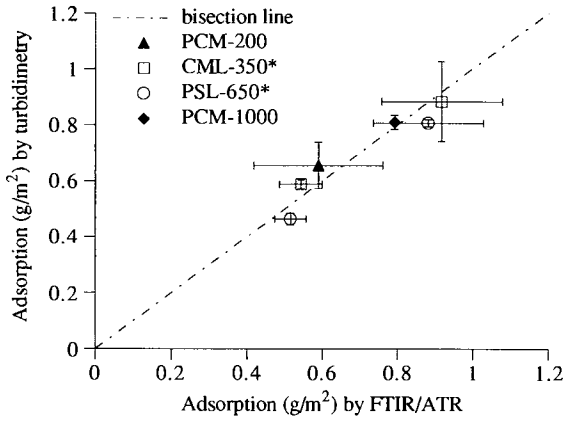

Fig. 3. Comparison of adsorption data obtained by turbidimetry and by FTIR-ATR. Bisection line, theoretical curve.

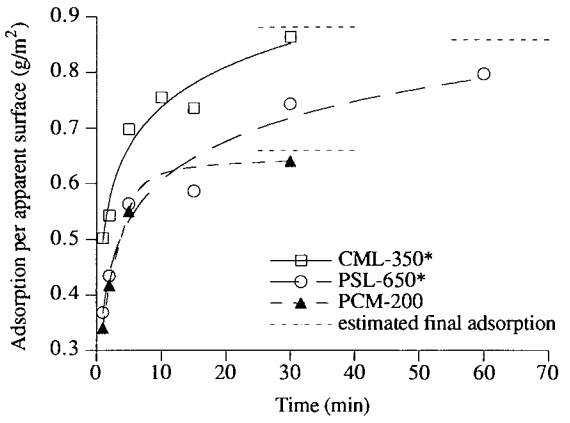

Fig. 4. Adsorption kinetics of latexes on rat intestinal mucosa. Bulk concentration of latex, 4 g/L; estimated final adsorption, plateaus of near-equilibrium adsorption isotherms (12).

where $q(t)$ is the coverage of the mucosa as a function of time and is given by

$$q(t) = (C_0 - C_t)/(C_0 - C_f) \qquad (2)$$

where C_0, C_t, and C_f are the latex concentrations in the suspension medium at time 0, time t, and in the final equilibrium, respectively. Substitution of Eq. (2) into Eq. (1) and subsequent integration (13) resulted in

$$\ln [C_t/(C_t - C_f)] = \ln [C_0/(C_0 - C_f)] + [C_f/(C_0 - C_f)]Kt \qquad (3)$$

The concentrations C_t and C_f were calculated as the differences between the initial latex bulk concentration in the suspension medium and the adsorbed latex amounts at time t and in the final equilibrium (Fig. 4), respectively. The rate constants K in the first phase of the adsorption kinetics were estimated from the plots of $\ln[C_t/(C_t - C_f)]$ against t (Fig. 5). The rate constants K found were 0.268 (min^{-1}) for PCM-200, 0.120 (min^{-1}) for CML-350*, and 0.044 (min^{-1}) for PSL-650*.

Influence of the Intestinal Region

Figure 6 shows the adsorption of latex PSL-650* ac-

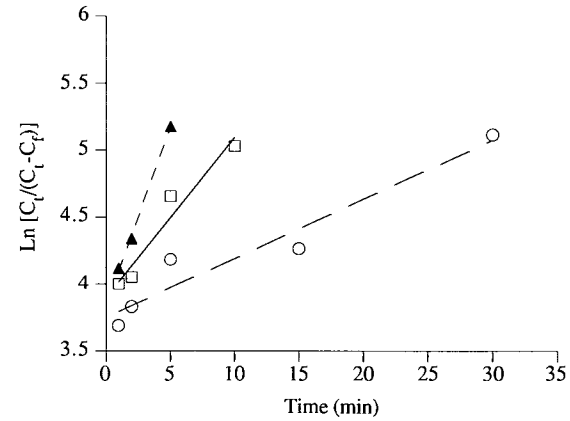

Fig. 5. Theoretical plots according to Eq. (3) for the experimental data given in Fig. 4.

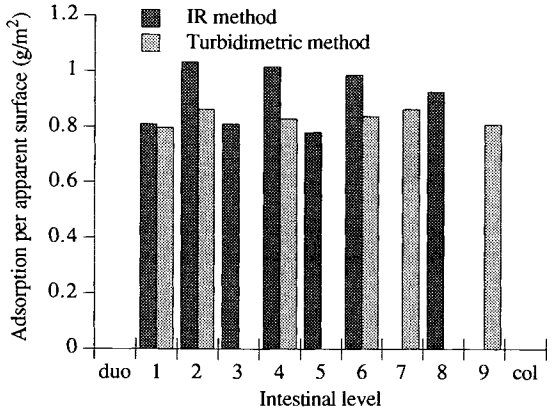

Fig. 6. Dependence of latex adsorption on the intestinal level in rat. Bulk concentration of PSL-650*, 4 g/L. duo, duodenum; col, colon.

cording to the intestinal level. No dependence on the intestinal level was found for the tested jejunum and ileum. The mean adsorption was 0.908 ± 0.107 for the IR values, 0.833 ± 0.072 for the turbidimetric values, and 0.873 ± 0.087 for all values. The ratio of turbidimetric values over IR values (ratio = 0.917) corresponded well to the ratio found in the comparison of the two methods (Table I).

DISCUSSION

FTIR-ATR Analysis

In the spectra of mucosa, the absorbance of carbonyl and methylene bands increased with higher sampling pressure because the scanning beam probably reached membrane lipids. This was supported by the estimation that the rat intestinal mucous layer, which consists typically of about 97.5% water (15) and has a mean thickness of about 80 μm under physiological conditions (16), in dry form might have a mean thickness of only about 2 μm. The penetration depth of the scanning IR beam in the sample was also about 2 μm at a frequency of 1500 cm^{-1} and for the ATR crystal used (17). Since the amide II peak and the poly(styrene) peak at 1493 cm^{-1} depended in the same manner on the sampling pressure, their use for dosage seemed appropriate. Further, the amide II band was sufficiently separated from the band of water still present in the sample, whereas the absorbance in the amide I band was modified by the water band (1640 cm^{-1}). In addition, the amide II band was reported to be relatively insensitive to changes in conformation of proteins (18). Another advantage of using two neighboring peaks for quantification was that they had the same dependence on the penetration depth of the IR beam in the sample (17,19).

Looking at the limited penetration depth of the scanning IR beam (17), it seemed necessary to estimate the thickness of the adsorbed latex layer. At 1.5 g/m^2, the latex layer has a mean thickness of 2.7 μm in a model of loose packing of spheres with 48% porosity between the particles and a thickness of 1.9 μm in a model of close packing with 26% porosity (20). Supposing close packing of the adsorbed particles in dried samples, it was proposed that the increase in the ratio (latex/mucus) with increasing latex adsorption was up to 1.5 g/m^2 due to both the increasing latex peak and the decreasing penetration of the scanning IR beam into the dried mucus under or between the particles. Therefore, IR dosage was valid up to 1.5 g/m^2.

Comparison of IR and Turbidimetric Analysis

The differences in the bisection line in Fig. 3 were not surprising for biological samples because they included variations between intestinal samples ($n \geq 3$) within one animal or several rats ($n \geq 2$). For example, the variation in the mean thickness of the mucous layer between samples from the same rat and in overall mean thickness between rats ranged up to twofold values (16). Since the penetration depth of the IR beam in the sample was of the same order as the thickness of the adsorbed latex layer or of the dried mucous layer when no or just a few particles were adsorbed, variations in thickness of the mucous layer may explain the larger standard deviations of the IR compared with the turbidimetric method. The IR results might also have been influenced by variation in the homogeneity of distribution of the adsorbed particles on the mucous layer. Incomplete denaturation of the mucus in turbidimetric samples was proposed as a reason for the differences between the experimental ratios and the bisection line. As a conclusion, the two methods should be considered complementary: the turbidimetric method has a better reproducibility (see error bars in Fig. 3) and is not limited by the thickness of the adsorbed layer, whereas by the IR technique, a direct detection of adsorbed unlabeled latex particles on the mucosa is possible.

Kinetics

Theoretically, the deposition of model colloids on well-defined solid surfaces involves two steps: transport and attachment. The transport of suspended Brownian particles is dominated by convection and diffusion (21), while the attachment is controlled by surface interactions (22). In the present study, no flow was applied to the system under investigation. Controlled hydrodynamic conditions without turbulence or convection of particles were therefore assumed. The electrolyte concentration of physiological saline used (154 mmol/L) was under the critical NaCl concentration where latex particles with a size up to 340 nm aggregate, but it was around the critical NaCl concentration where reversible flocculation of larger particles may occur (23). On the other hand, it was found that the latexes studied here started to agglomerate at latex concentrations of about 15 g/L in physiological saline (12). Therefore, particle/particle interactions in the suspension medium were neglected for the present work. Further, in physiological saline, the absence of an energy barrier was accepted (22,24). Thus, the control of the adsorption rate was attributed to the Brownian motion of the particles. The diffusion rate in the latex suspension was described according to the first Fickian law of diffusion:

$$dm/dt = -DA(dC/dx) \quad (4)$$

where the mass dm, which reaches the area A in the time dt, is directly proportional to the gradient of concentration dC over the distance $dx(-dC/dx)$. D is the diffusion coefficient, which is described by the Stokes–Einstein equation:

$$D = kT/6\pi\eta r \quad (5)$$

where k is the Boltzmann's constant, T the absolute temperature, η the viscosity of the suspension medium, and r the radius of the particle.

To explain the different rates of adsorption, the parameters influencing the diffusion in the suspension medium were analyzed. The apparent surface A of the adsorbent, the temperature T, and the initial latex concentration C were equal for all kinetic studies. When mucus is exposed to an excess of physiological saline, it remains as a separate gel phase instead of dispersing (25,26). Therefore, constant η was assumed in the suspension medium. Looking at the radius r of the adsorbates, the expected adsorption rate would be two and three times slower for PSL-650* than for CML-350* and PCM-200, respectively. The observed rate constants K were three and six times smaller for PSL-650* than for CML-350* and PCM-200, respectively. These larger differences suggested that the kinetics of adsorption depended beside the diffusion in the suspension medium on other parameters. Classically, it was proposed that adsorption kinetics were controlled by the phase of attachment which followed the transport phase. The attachment may be described by the DLVO theory and depend on London–van der Waals attraction and electrical double-layer repulsion (21). However, since the mucous gel constitutes a porous rather than a smooth adsorbent (12), the adsorption kinetics may be controlled in a second phase of transport by diffusion in the mucus network (27).

Influence of the Intestinal Region

Since the aim of this study was to compare different latexes, it was a must to verify that the results were not influenced by variations of the mucosa samples. As previously mentioned, Peyer's patches were avoided in this study. So their density of distribution in the intestine did not interfere. Although no obvious correlation between the mucous gel thickness and the distance from the pylorus was revealed, variations in its thickness were reported (16). In this study, the variation in adsorption (SD = 10.0% for all values) was much less important than the reported changes in mucus thickness. Thus, the mucous gel layer of rat jejunum and ileum was considered homogeneous, and adsorption data on samples from jejunum and ileum could be compared with each other.

CONCLUSION

A new model to evaluate mucoadhesion of latexes under static conditions as well as two methods for quantifying the adsorption was developed. The comparison of this new application of the FTIR-ATR technique with the turbidimetric analysis gave good agreement. The first phase of the adsorption kinetics of three latexes with different particle size was approached by a physical model of diffusion in the suspension medium. The intestinal level of the mucosa sample did not interfere with the adsorption studies for the tested jejunum and ileum.

ACKNOWLEDGMENTS

C. Durrer thanks the Roche Research Foundation, Basel, Switzerland, for the grant that enabled him to conduct this research during his doctoral studies at the University of Paris Sud. We thank Mr. E. Chipon and F. Delène Mirouze, Unicam, Argenteuil, France, for their advice and criticism.

REFERENCES

1. J. R. Robinson. Rationale of Bioadhesion/Mucoadhesion. In R. Gurny and H. E. Junginger (eds.), *Bioadhesion-Possibilities and Future Trends*, Wissenschaftliche Verlagsgesellschaft, Stuttgart, 1990, pp. 13–15.
2. S. Wu. *Polymer Interface and Adhesion*, Marcel Dekker, New York, 1982.
3. G. Ponchel, F. Touchard, D. Duchêne, and N. A. Peppas. Bioadhesive analysis of controlled-release systems. I. Fracture and interpenetration analysis in poly(acrylic acid)-containing systems. *J. Control. Rel.* 5:129–141 (1987).
4. G. Ponchel, F. Touchard, D. Wouessidjewe, D Duchêne, and N. A. Peppas. Bioadhesive analysis of controlled-release systems. III. Bioadhesive and release behavior of metronidazole-containing poly(acrylic acid)-hydroxypropyl methylcellulose systems. *Int. J. Pharm.* 38:65–70 (1987).
5. K. V. Rango Rao and P. Buri. A novel *in situ* method to test polymers and coated microparticles for bioadhesion. *Int. J. Pharm.* 52:265–270 (1989).
6. C. Pimienta, V. Lenaerts, C. Cadieux, P. Raymond, J. Juhasz, M. A. Simard, and C. Jolicoeur. Mucoadhesion of hydroxypropylmethacrylate nanoparticles to rat intestinal ileal segments *in vitro*. *Pharm. Res.* 7:49–53 (1990.
7. C. L. C. Teng and N. F. H. Ho. Mechanistic studies in the simultaneous flow and adsorption of polymer-coated latex particles on intestinal mucus. I. Methods and physical model development. *J. Control. Rel.* 6:133–149 (1987).
8. J. M. Irache, C. Durrer, G. Ponchel, and D. Duchêne. Determination of particle concentration in latexes by turbidimetry. *Int. J. Pharm.* 90:R9–R12 (1993).
9. P. K. Gupta, S. H. S. Leung, and J. R. Robinson. Bioadhesives/mucoadhesives in drug delivery to the gastrointestinal tract. In V. Lenaerts and R. Gurny (eds.), *Bioadhesive Drug Delivery Systems*, CRC Press, Boca Ragon, FL, 1990, pp. 65–92.
10. C. Durrer, G. Ponchel, and D. Duchêne. Detection of polymer latexes at mucosal surface by Fourier transform infrared/attenuated total reflectance spectroscopy (FT-IR/ATR). *6th Congr. Int. Technol. Pharm.* 2:66–73 (1992).
11. J. F. Forstner, I. Jabbal, and G. G. Forstner. Goblet cell mucin of rat small intestine. Chemical and physical characterization. *Can. J. Biochem.* 51:1154–1166 (1973).
12. C. Durrer, J. M. Irache, F. Puisieux, D. Duchêne, and G. Ponchel. Mucoadhesion of latexes. II. Adsorption isotherms and desorption studies. *Pharm. Res.* 11:680–683 (1994).
13. B. Vincent, M. Jafelicci, P. f. Luckham, and T. F. Tadrow. Adsorption of small, positive particles onto large, negative particles in the presence of polymer. 2. Adsorption equilibrium and kinetics as a function of temperature. *J. Chem. S. Faraday I* 76:674–682 (1980).
14. P. R. Rutter and B. Vincent. Physicochemical interactions of the substratum, microorganisms, and the fluid phase. In K. C. Marshall (ed.), *Microbial Adhesion and Aggregation*, Dahlem Konferenzen, Springer-Verlag, Berlin, 1984, pp. 21–38.
15. J. M. Creeth. Constituents of mucus and their separation. *Br. Med. Bull.* 34:17–24 (1978).
16. S. McQueen, D. Hutton, A. Allen, and A. Garner. Gastric and duodenal surface mucus gel thickness in rat: Effects of prostaglandins and damaging agents. *Am. J. Physiol.* 245:G388–G393 (1983).
17. R. Iwamoto and K. Ohta. Quantitative surface analysis by Fourier transform attenuated total reflection infrared spectroscopy. *Appl. Spectrosc.* 38:359–365 (1984).
18. R. J. Jakobsen and F. M. Wasacz. Infrared spectra—Structure correlations and adsorption behavior for helix proteins. *Appl. Spectrosc.* 44:1478–1490 (1990).
19. F. M. Mirabella. Quantitative aspects of internal reflection spec-

troscopy: Polymer surface composition measurement. *J. Polym. Sci.* 23:861–871 (1985).
20. A. N. Martin, J. Swarbrick, and A. Cammarata. *Physikalische Pharmazie: pharmazeutisch angewandte physikalisch-chemische Grundlagen,* H. Stricker (ed.), Wissenschaftliche Verlagsgesettschaft, Stuttgart, 1987.
21. M. Elimelech and C. R. O'Melia. Effect of particle size on collision efficiency in the deposition of Brownian particles with electrostatic energy barriers. *Langmuir* 6:1153–1163 (1990).
22. T. F. Tadros. Particle-surface adhesion. In R. C. W. Berkeley, J. M. Lynch, J. Melling, P. R. Rutter, and B. Vincent (eds.), *Microbial Adhesion to Surfaces,* Society of Chemical Industry, Ellis Horwood, Chichester, England, 1980, pp. 93–116.
23. G. C. Jeffrey and R. H. Ottewill. Reversible aggregation. I. Reversible flocculation monitored by turbidity measurements. *Colloid Polym. Sci.* 266:173–179 (1988).
24. M. Hull and J. A. Kitchener. Interaction of spherical colloidal particles with planar surfaces. *Trans. Faraday Soc.* 65:3093–3104 (1969).
25. A. Allen, A. Bell, M. Mantle, and J. P. Pearson. The structure and physiology of gastrointestinal mucus. *Adv. Exp. Med. Biol.* 144:115–133 (1982).
26. F. A. Meyer. Mucus structure: Relation to biological transport function. *Biorheology* 13:49–58 (1976).
27. N. A. Peppas, P. J. Hansen, and P. A. Buri. A theory of molecular diffusion in the intestinal mucus. *Int. J. Pharm.* 20:107–118 (1984).